Saudi Journal of Biological Sciences 28 (2021) 7336–7348

Contents lists available at ScienceDirect

Saudi Journal of Biological Sciences

journal homepage: www.sciencedirect.com

Original article

Significant transcriptomic changes are associated with the inhibitory effects of 5-aza-2-deoxycytidine during adipogenic differentiation of MG-63 cells

Amir Ali Khan [a,b,*], Muhammad Nasir Khan Khattak [a,b], Divyasree Parambath [c], Ahmed Taher El-Serafi [c,d,e,*]

[a] Department of Applied Biology, College of Sciences, University of Sharjah, Sharjah 27272, United Arab Emirates
[b] Human Genetics and Stem Cells Research Group, Research Institute of Sciences & Engineering (RISE), University of Sharjah, Sharjah 27272, United Arab Emirates
[c] Sharjah Institute for Medical and Health Research, University of Sharjah, Sharjah 27272, United Arab Emirates
[d] Department of Biomedical and Clinical Sciences (BKV), Linköping University, P.O. Box 581 83, Linköping, Sweden
[e] Medical Biochemistry department, Faculty of Medicine, Suez Canal University, 41522, Ismailia, Egypt

ARTICLE INFO

Article history:
Received 11 June 2021
Revised 25 July 2021
Accepted 12 August 2021
Available online 19 August 2021

Keyword:
Adipogenesis
Transcriptomics analysis
MG-63 cells
Suberoylanilide hydroxamic acid
5-Aza-2-deoxycytidine

ABSTRACT

Our previous study revealed that the treatment of 5-aza-2-deoxycytidine (5-aza) inhibited while treatment of suberoylanilide hydroxamic acid (SAHA) enhanced the adipogenic differentiation of MG-63 cells. In this study, we examined the transcriptomic profiles of the derived adipocyte-like cells from MG-63 cells in the presence of 5-aza (Treatment 1) and SAHA (Treatment 2). Genome wide expression analysis showed high within sample variability for the adipocytes derived with 5-aza versus vehicle. Additionally, the expression profile of 5-aza derived cells was separated from the other sample groups. Differential analysis on the pairwise comparison of 5-aza versus control and SAHA versus 5-aza identified 1290 and 1086 differentially expressed (DE) genes, respectively. Furthermore, some overlap was observed between the up and down-regulated DE genes of 5-aza versus control and SAHA versus control (jaccard score 0.3) as well as between the differentially regulated genes of 5-aza versus control and 5-aza versus SAHA (jaccard score 0.29). A total of 73 transcription factors (TFs) were differentially expressed across all the pair wise comparisons with some overlap between the under and over expressed TFs of 5-aza versus control and 5-aza versus SAHA (jaccard score 0.29). Unsupervised clustering of TFs showed that the samples within the group are consistent in expression and the samples cluster in accordance with the group.

Several GO terms related to enhanced adipogenesis such as neutral lipid biosynthetic process, lipid metabolic processes, cellular amide metabolic processes and cellular carbohydrate metabolic processes were enriched in the down regulated genes of 5-aza derived adipocytes versus control, indicating 5-aza inhibit the adipogenic differentiation of MG-63 cells. GSEA analysis on selected gene sets of MAPK and PI3K signaling pathway in MSigDB identified the pathways were up-regulated in 5-aza versus control. This study revealed that inhibition of MG-63 adipogenesis due to 5-aza treatment is associated with large transcriptomics changes and further research is needed to unravel the roles of these genes in the adipogenesis.

1. Introduction

Obesity is pandemic and more population are suffering from the disorder in the developed countries. It is essential to know the molecular mechanisms that are responsible for adipogenesis. Suberoylanilide hydroxamic acid (SAHA) inhibits the histone deacetylases enzymes and inhibition of these enzymes prevent the acetyl groups removal from histones. The acetylation of histone relaxes the interaction of histone with DNA thereby enhances the transcription (Roth and Allis, 1996; Jones and Takai, 2001). The application of HDAC inhibitors is usually associated with enhanced

* Corresponding authors at: Department of Applied Biology, College of Sciences, University of Sharjah, Sharjah 27272, United Arab Emirates (A.A. Khan). Sharjah Institute for Medical and Health Research, University of Sharjah, Sharjah 27272, United Arab Emirates (A.T. El-Serafi).
E-mail address: amkhan@sharjah.ac.ae (A.A. Khan).

Peer review under responsibility of King Saud University.

Production and hosting by Elsevier

https://doi.org/10.1016/j.sjbs.2021.08.033
1319-562X/

expression of certain genes that may induce stem cell differentiation as well as cellular determination and commitment during development. Histone deacetylase (HDAC) inhibitors induce cell cycle arrest (Sandor et al., 2000); regulate apoptosis (Kim and Bae, 2011) and affects signaling pathways (Blaheta and Cinatl, 2002; Yuan et al., 2001).

HDACs inhibitors also regulate somatic cells differentiation into induced pluripotent stem cells (Higuchi et al., 2015). As acetylation of histone relaxes the interaction between histone and DNA, histone acetylation leads to activation of related genes. Interestingly, histone acetylation is expected to affect 2–10% of all genes in a cell (Mariadason et al., 2000). Hence the differential regulation of these genes affects the derivation of induced pluripotent stem cells or the differentiation into certain lineages.

5-Aza-2-deoxycytidine (5-aza) is a DNA methylation inhibitor and regulate genes that are responsible for derivation of mature cell types. One the other hand, genes that regulate the histone modifications are involved in early development. DNA methylation changes is one of the mechanisms that regulate gene expression without changes in DNA sequences (Jones and Takai, 2001). Furthermore, DNA methylation inhibitor has also roles in stem cells reprogramming. DNA demethylation may lead to the activation of silent genes that may affect stem cells differentiation. The reprograming of somatic cells into induced pluripotent cells was reported to be regulated by DNA methylation (Chen et al., 2015).

Several studies have reported that 5-aza regulates the stem cells differentiation. For example, 5-aza enhanced the differentiation of mesenchymal stem cells into the osteoblastic lineage as well as insulin secreting cells (El-Serafi et al., 2011; Elsharkawi et al., 2020).

In our previous study, we reported that HDAC inhibitor enhances while 5-aza inhibits the differentiation of adipocytes from MG-63 cells (El-Serafi et al., 2019). MG-63 is osteosarcoma cell line and has analogous differentiation potential as of mesenchymal stem cells.

To unravel the molecular mechanisms of the enhanced and inhibited differentiation of MG-63 cells into adipocytes with SAHA and 5-aza respectively, the transcriptomic profiles of adipocytes were compared derived with treatment of the two epigenetic modifiers.

mRNA sequencing is a robust method and can unravel many genes that are differentially expressed (Khan et al., 2020). Hence, we have investigated the transcriptomics of adipocytes derived with and without the treatments of 5-aza and SAHA by mRNA sequencing. This method has identified the genes that are involved in the enhanced and inhibited differentiation of adipocytes which may be possible therapeutic targets in the treatment of obesity.

2. Methods and material

2.1. mRNA samples

mRNA samples extracted from MG-63 derived adipocyte-like cells as described in our earlier study (El-Serafi et al., 2019), were sent for mRNA sequences. The Fig. 1 depicts the flow diagram of the experiment. MG-63 cells were differentiated in the presence of 5-aza (treatment 1), SAHAH (treatment 2), Vehicle (DMSO) and control (PBS).

2.2. Total RNA extraction and illumina cDNA library preparation

The mRNA stranded library was prepared and Nextseq®500 Sequencing System (Illumina, CA, USA) was used to perform mRNA sequencing according to the manufacturer's instructions. The sequencer was set to perform a double-end sequence of 25 M reads per sample.

2.3. Read pre-processing, QC, alignment and gene quantification

Prior to differential expression (DE) analysis, all the raw reads were analyzed for contamination and sequencing quality. Any trimming was done with BBDuk and subsequently reads were aligned to latest reference genome (rn6) with GTF from Ensembl (v99) using STAR aligner (Dobin et al., 2013). Aligned reads were transformed into read counts per gene by RSEM tool (Li and Dewey, 2011).

2.4. Differential expression analysis

Pairwise differential expression analysis was done with DESeq2 R package (Love et al., 2014) with control samples were used as reference for individual experiments, except for the comparison between 5-aza treatment and SAHA treatment where 5-aza treatment was used as the reference. The expression counts were scaled and normalized to correct the sequencing depth and batch differences among the samples. These normalized counts were then used for differential expression analysis. Fold change values were generated in log2 scale [log2(sample/control)] for contrasts 5-aza

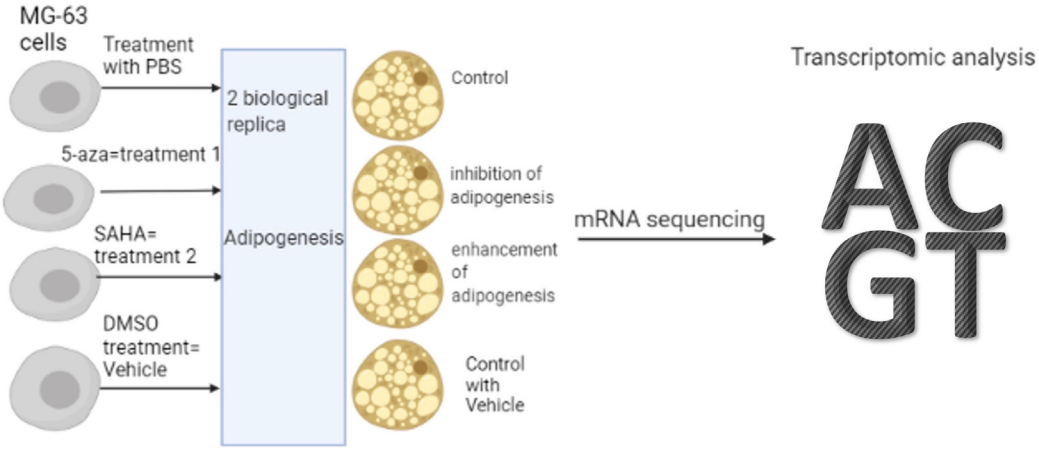

Fig. 1. Schematic diagram illustrating the plan of the study. Before adipogenic differentiation, MG-63 cells were treated with PBS (control), 5-Aza (treatment 1), SAHA (treatment 2) and DMSO (vehicle) for three consecutive days. The treated MG-63 cells were then differentiated into adipocytes-likes cells and mRNAs were extracted from the derived adipocytes for mRNA sequencing. mRNAs were sequenced from the pair ends and further data analysis was performed.

treatment (treatment 1) versus control, SAHA derived adipocytes (treatment 2) versus control, vehicle versus control and SAHA treatment (treatment 2) versus 5-aza treatment (treatment 1). Genes having lower read count can generate higher values of fold change; this may lead to possible false positives. For this reason, the fold changes that were risen due to ratio between lower read counts in samples were adjusted by employing fold change shrinkage estimator approach from DESeq2. Genes with adjusted p value ≤ 0.05 and log2 fold change of +1 or −1 were considered as significantly up and down-regulated genes respectively.

2.5. GO enrichment analysis

GO analysis was performed on differentially regulated genes from different analysis with the Cytoscape v3.6.1 (Shannon et al., 2003) plug-in ClueGO v2.5.5 (Bindea et al., 2009). Statistically enriched biological processes (updated on 20/05/2019) were functionally grouped according to their k-score, and the most significant GO term of each group was used as summarizing GO term for the group.

2.6. GSEA analysis

GSEA was performed as described earlier (Subramanian et al., 2005) against the selected gene sets from MAPK and PI3K signaling in MSigDB with the ranking metric Signal2noise with 1000 geneset permutations for statistical assessment of enrichment. Only terms with an FDR ≤ 0.25 were considered significant.

2.7. Pathway analysis

Pathway analysis was done with Reactome analysis tool (Fabregat et al., 2017) for both up and down-regulated genes. Pathways with FDR ≤ 0.05 were considered statistically significant.

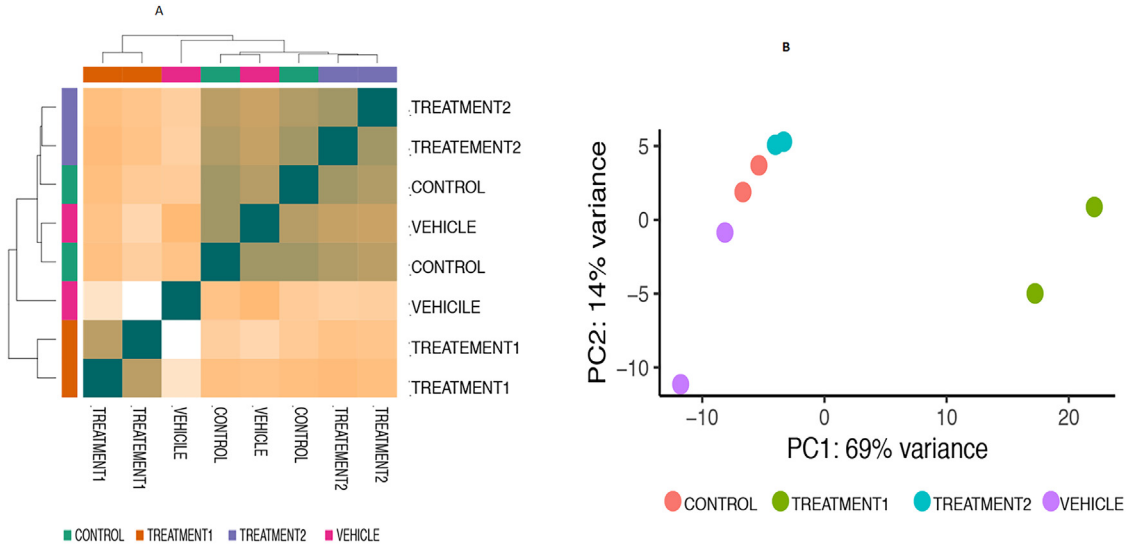

Fig. 2. (a) Principal component analysis (PCA) plot of samples: Samples are color coded based on their group. PCA method was applied to assess the clustering of the samples based on similarity. Results above show that the treatment1 (5-aza) samples are well separated from the groups control and vehicle. (b) Unsupervised Hierarchical Sample clustering: To illustrate the distance between samples and replicates, samples were clustered (hierarchical) based on the sample distance. This distance was calculated from the dispersion rate of gene expression. Results show that the treatment 1 (5-aza) samples cluster together and are separated from the groups control, vehicle and treatment 2 (SAHA).

Table 1
List of top 20 significantly differentially expressed genes (treatment 1 versus control).

Ensembl	Gene type	Genes symbol	Log2 FoldChange	Adjusted P-value
ENSG00000110446.11	protein_coding	SLC15A3	5.34	2.85E−14
ENSG00000107159.13	protein_coding	CA9	−3.74	2.66E−09
ENSG00000134321.12	protein_coding	RSAD2	3.72	1.42E−62
ENSG00000163347.6	protein_coding	CLDN1	5.12	7.25E−53
ENSG00000187608.10	protein_coding	ISG15	3.31	5.73E−29
ENSG00000211445.12	protein_coding	GPX3	3.29	7.80E−70
ENSG00000183486.13	protein_coding	MX2	3.51	4.42E−35
ENSG00000235288.3	lncRNA	AC099329.1	7.91	9.95E−04
ENSG00000100889.12	protein_coding	PCK2	−3.19	1.82E−46
ENSG00000070669.17	protein_coding	ASNS	−3.18	4.01E−73
ENSG00000163739.5	protein_coding	CXCL1	3.91	6.51E−25
ENSG00000157601.14	protein_coding	MX1	3.13	5.07E−53
ENSG00000204379.11	protein_coding	XAGE1A	8.33	3.44E−06
ENSG00000119917.14	protein_coding	IFIT3	3.06	1.58E−64
ENSG00000196616.14	protein_coding	ADH1B	−3.43	2.63E−34
ENSG00000168209.5	protein_coding	DDIT4	−3.02	4.06E−42
ENSG00000123689.6	protein_coding	G0S2	−3.04	9.46E−24
ENSG00000165949.12	protein_coding	IFI27	2.90	2.68E−49
ENSG00000149591.17	protein_coding	TAGLN	3.74	2.25E−04
ENSG00000078401.7	protein_coding	EDN1	2.99	1.32E−31

2.8. Transcription factor analysis

Genes reported to function as transcription factors were downloaded from TFcheckpoint database (Chawla et al., 2013) and reported entrez gene ids were converted to corresponding Ensembl ids using Ensembl Biomart.

3. Results

3.1. Genome-wide expression profiling

Fig. 1 depicts the study design of the study. The mapping and quality statistics of the data is given in supplementary information 1. We assessed the overall similarity between the replicates using Principal Component Analysis (PCA) (Fig. 2A) and unsupervised hierarchical clustering using distance matrix (Fig. 2B).

Overall, the result shows that the Treatment 1 (5-aza) are well separated from all the groups. There is some variability within the two groups – Treatment1 and the Vehicle. Given these observations all the differential analysis was hence performed as pairs instead of all groups together.

3.2. Transcriptomic analysis of 5-aza derived adipocytes versus control adipocytes (treatment 1 versus control)

3.2.1. Differentially expressed genes expressed

A total of 1, 290 genes are differentially expressed (Table 1 and supplementary information 2) with a comparable number of up

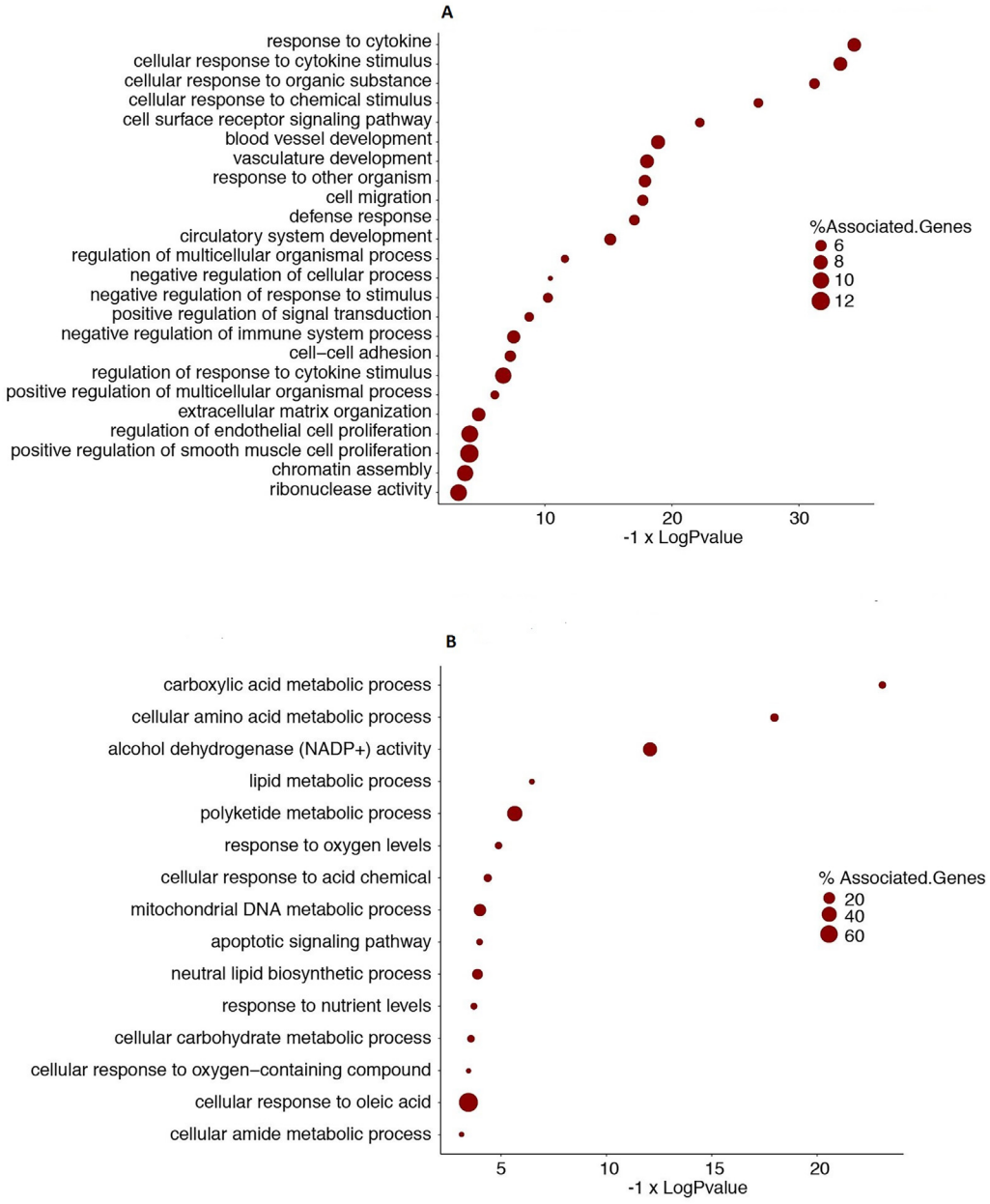

Fig. 3. (A) GO terms enriched in upregulated genes in adipocytes derived with Treatment 1 (5-aza) versus control adipocytes. Hypergeometric test was performed on the upregulated genes in adipocytes derived with 5-aza to find GO terms that are significantly enriched. They are shown in y-axis and the associated adjusted p-value (Bonferroni step down) are reported in x-axis. Size of the dots shows the percentage of genes associated with the GO term identified in the up-regulated genes. (B) GO terms enriched in down regulated genes in adipocytes derived with Treatment 1 versus control. Hypergeometric test was also performed on down regulated genes adipocytes derived with 5-aza to find statistically significant GO terms. These GO terms are shown in y-axis and the associated adjusted p-value (Bonferroni step down) are reported in x-axis. Size of the dots represent the percentage of genes associated with the GO term identified in the down-regulated genes.

Table 2
List of significantly enriched pathways and biological process with 5-aza pretreatment (treatment 1), in comparison to the control. ES and NES refers to enrichment score and normalized enrichment score respectively.

MSigDB Gene Set	SIZE	ES	NES	FDR q-val
GO_ACTIVATION_OF_MAPK_ACTIVITY	149	0.62	1.36	0.10
GO_POSITIVE_REGULATION_OF_MAP_KINASE_ACTIVITY	256	0.61	1.37	0.10
GO_INACTIVATION_OF_MAPK_ACTIVITY	27	0.78	1.41	0.11
PID_PI3K_PLC_TRK_PATHWAY	36	0.69	1.32	0.12
GO_REGULATION_OF_MAP_KINASE_ACTIVITY	334	0.61	1.38	0.12
GO_ACTIVATION_OF_MAPKK_ACTIVITY	54	0.66	1.32	0.14
GO_NEGATIVE_REGULATION_OF_MAP_KINASE_ACTIVITY	77	0.69	1.43	0.15
REACTOME_CONSTITUTIVE_SIGNALING_BY_ABERRANT_PI3K_IN_CANCER	75	0.62	1.27	0.16
GO_PHOSPHATIDYLINOSITOL_3_KINASE_SIGNALING	147	0.56	1.22	0.24

(667) and down-regulated (623) genes in adipocytes derived with 5-aza compared with control. The top 20 significantly differentially expressed genes are listed in Table 1. All of the differentially regulated genes are listed in supplementary information 2.

3.2.2. GO enrichment analysis

Non-redundant GO terms, post semantics similarity, that are significantly over represented in the list of up and down regulated genes in 5-aza treatment are shown in Fig. 3A and B respectively.

3.2.3. GSEA enrichment analysis

GSEA analysis identified 9 pathways / biological process from selected gene sets of MAPK and PI3K signaling from MSigDB that are enriched and up-regulated in 5-aza treatment (Table 2 and Fig. 4) on the expression dataset of 5-aza treatment versus Control.

3.2.4. Pathway enrichment analysis

Pathway enrichment analysis identified 16 significantly (≤0.05 FDR) overrepresented pathways in the Reactome database for up-regulated genes in 5-aza treatment, treatment 1, (Fig. 5). However, for the down-regulated genes no pathways were significantly enriched.

3.2.5. Transcription factor analysis

A total 59 transcription factors (TFs) are differentially expressed: 33 were upregulated in 5-aza treatment, treatment 1, while 26 were downregulated (Supplementary information 2).

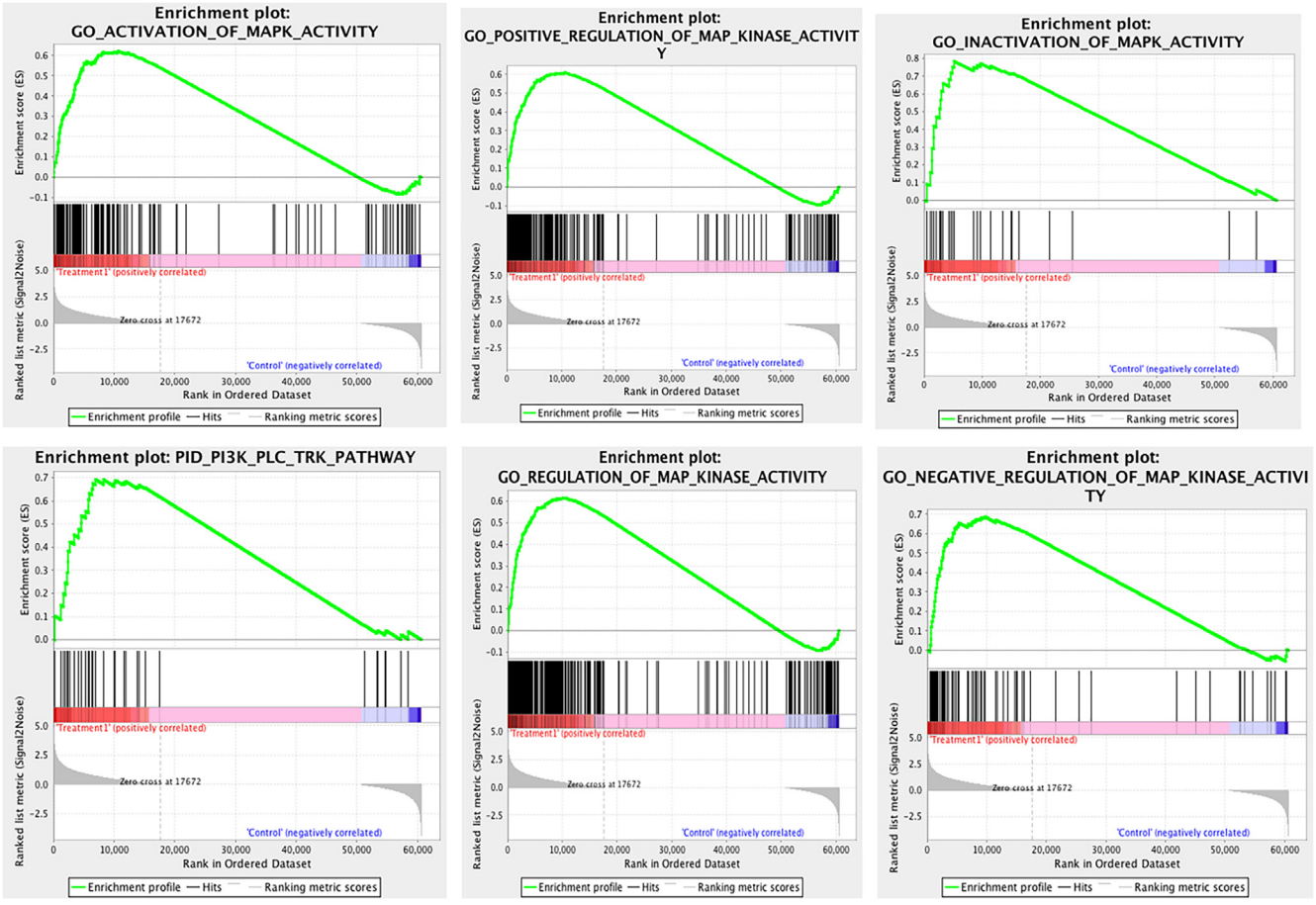

Fig. 4. Gene set enrichment analysis: Top 6 significantly enriched gene sets from the list of selected MAPK and PI3K signaling gene sets of MSigDB up-regulated in phenotype Treatment 1 (5-aza) are reported for gene expression analysis of Treatment 1 versus Control.

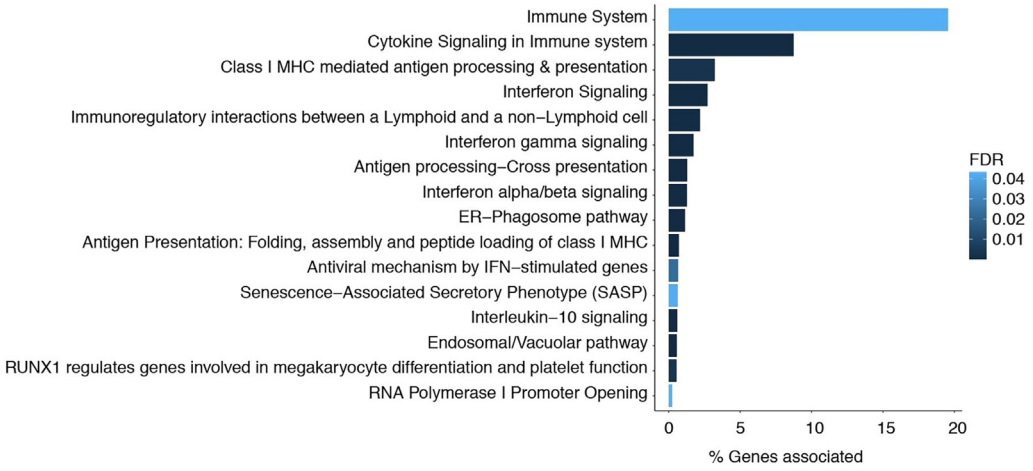

Fig. 5. Pathways enrichment in upregulated genes in adipocytes derived with treatment 1 (5-aza) versus control adipocytes. Shown are the pathways in Reactome database significantly enriched for upregulated genes in Treatment 1 (5-aza). Pathway names are shown in the y-axis and the percentage of genes associated with the enriched pathway are reported in the x-axis. Colour gradient corresponds to FDR.

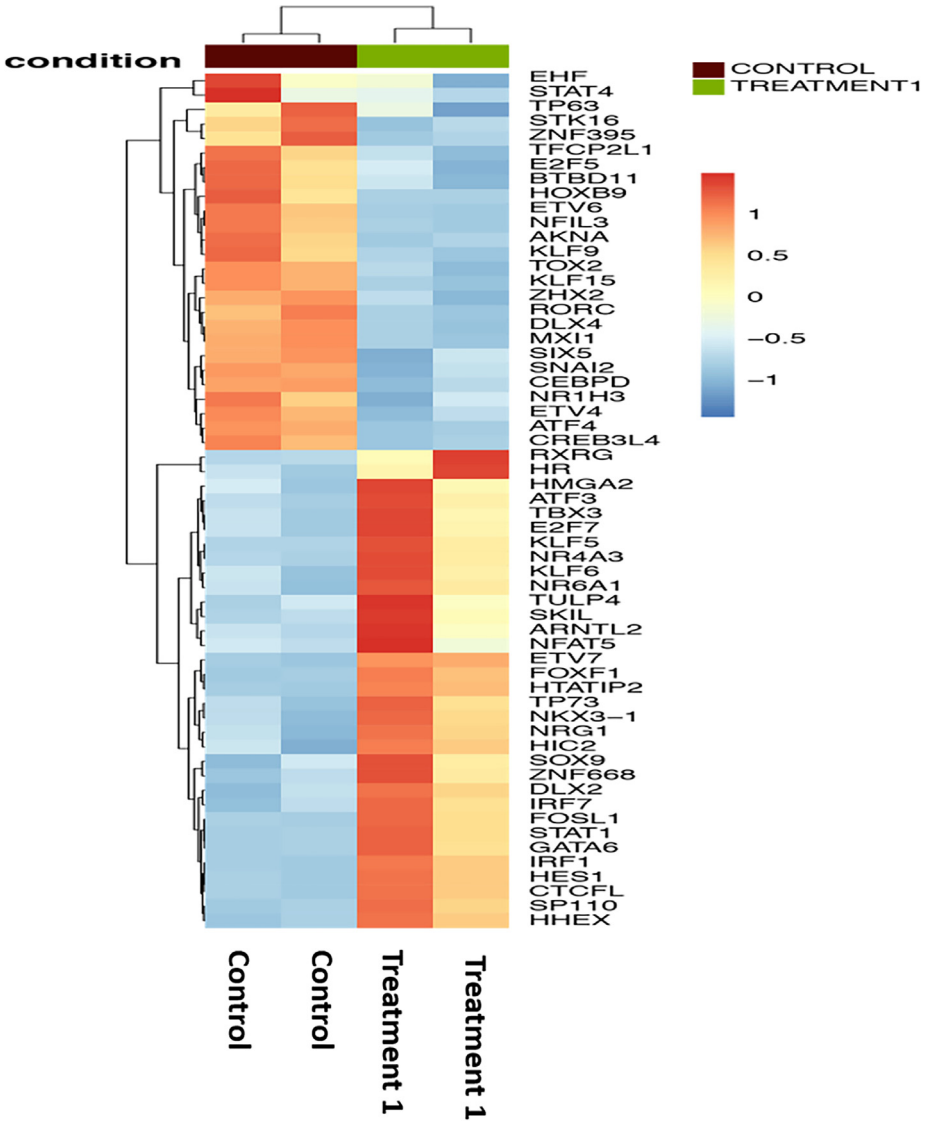

Fig. 6. Hierarchical clustering of differentially expressed transcription factors between control and treatment 1 (5-aza) derived adipocytes. Differentially expressed and statistically significant transcription factors are shown. The color scale bar indicates z-score values after z-score row normalization. Heatmap was generated using pheatmap package from R.

Table 3
List of significantly differentially expressed genes (Treatment 2 versus Control).

Ensembl	Gene type	Genes symbol	Log2 FoldChange	Adjusted P-value
ENSG00000135744.8	protein_coding	AGT	−1.88	6.65E−26
ENSG00000196275.14	protein_coding	GTF2IRD2	−3.08	5.23E−08
ENSG00000180071.20	protein_coding	ANKRD18A	3.83	8.20E−04
ENSG00000261771.5	lncRNA	DNAAF4-CCPG1	−9.15	1.09E−05
ENSG00000283765.1	protein_coding	AC131160.1	8.01	3.91E−04
ENSG00000242288.9	lncRNA	AC022400.3	8.26	2.49E−04
ENSG00000224597.10	transcribed unprocessed pseudogene	SVIL-AS1	1.49	5.50E−08
ENSG00000137869.15	protein_coding	CYP19A1	−1.42	2.32E−04
ENSG00000229314.5	protein_coding	ORM1	−1.18	2.70E−06
ENSG00000249967.1	protein_coding	AL355315.1	5.19	4.08E−02
ENSG00000257315.2	protein_coding	ZBED6	1.34	1.04E−03
ENSG00000243414.5	protein_coding	TICAM2	−1.14	7.92E−03
ENSG00000129988.6	protein_coding	LBP	−1.43	3.74E−02
ENSG00000196616.14	protein_coding	ADH1B	−1.01	1.73E−05

Table 4
Summary statistics of differentially regulated genes (Vehicle versus control).

Ensembl	Gene type	Genes symbol	Log2 FoldChange	Adjusted P-value
ENSG00000285053.1	protein_coding	TBCE	−2.40	5.51E−06
ENSG00000260537.2	protein_coding	AC012184.2	−8.17	1.18E−02
ENSG00000261771.5	lncRNA	DNAAF4-CCPG1	−8.99	1.44E−04
ENSG00000257315.2	protein_coding	ZBED6	−8.86	1.81E−04
ENSG00000151967.18	protein_coding	SCHIP1	−6.10	3.58E−02
ENSG00000288534.1	protein_coding	AP001931.2	−1.52	2.64E−02

Unsupervised clustering of TFs (Fig. 6) shows that the samples within the group are consistent in expression and the samples cluster in accordance with the group.

3.3. Transcriptomics analysis of SAHA derived adipocytes versus control (Treatment 2 versus Control)

3.3.1. Differentially expressed genes

A total 14 genes are differentially expressed (6 up and 8 down) in adipocytes derived with SAHA. The significantly differentially expressed genes are shown in Table 3.

3.3.2. Enrichment analysis

Neither any GO term, nor any pathway was significantly enriched in the differentially regulated genes. No selected MAPK and PI3K signaling gene sets from the MSigDB was enriched in any of the phenotypes – Treatment 2 and Control. Furthermore, there was not any known transcription factors present among the differentially expressed genes.

3.4. Transcriptomics analysis of adipocytes derived with DMSO and control (Vehicle versus control)

3.4.1. Differentially expressed genes

A total 8 genes are differentially expressed; 2 were up and 6 were down regulated in vehicle. The significantly differentially expressed genes are shown in table 4.

3.4.2. Enrichment analysis

Not any significantly enriched GO term was found in the differentially expressed genes.

Table 5
List of differentially expressed genes (Treatment 2 versus Treatment 1).

Ensembl	Gene type	Genes ymbol	Log2 FoldChange	Adjusted P-value
ENSG00000183486.13	protein_coding	MX2	−4.71	1.97E−57
ENSG00000211445.12	protein_coding	GPX3	−3.83	1.36E−83
ENSG00000110446.11	protein_coding	SLC15A3	−7.51	1.70E−15
ENSG00000157601.14	protein_coding	MX1	−3.37	5.73E−57
ENSG00000163347.6	protein_coding	CLDN1	−4.81	2.43E−49
ENSG00000134321.12	protein_coding	RSAD2	−3.31	2.65E−45
ENSG00000108691.9	protein_coding	CCL2	−3.27	6.93E−58
ENSG00000204379.11	protein_coding	XAGE1A	−8.26	5.74E−06
ENSG00000070669.17	protein_coding	ASNS	3.03	3.00E−65
ENSG00000149591.17	protein_coding	TAGLN	−3.95	6.85E−24
ENSG00000168209.5	protein_coding	DDIT4	2.98	2.78E−42
ENSG00000126709.15	protein_coding	IFI6	−2.98	6.23E−61
ENSG00000163993.7	protein_coding	S100P	−3.49	4.53E−08
ENSG00000100889.12	protein_coding	PCK2	2.83	1.06E−35
ENSG00000187608.10	protein_coding	ISG15	−2.78	3.53E−29
ENSG00000117525.14	protein_coding	F3	−2.93	1.18E−20
ENSG00000163739.5	protein_coding	CXCL1	−3.32	8.48E−21
ENSG00000165949.12	protein_coding	IFI27	−2.74	1.74E−49
ENSG00000170627.11	protein_coding	GTSF1	−6.06	1.25E−04
ENSG00000078401.7	protein_coding	EDN1	−2.88	1.00E−27

Only Post–chaperonin tubulin folding pathway (FDR 0.036) was enriched for down-regulated genes in Vehicle; no known transcription factors were present among the differentially expressed genes.

3.5. Transcriptomics analysis of SAHA derived adipocytes versus 5-aza derived adipocytes (Treatment 2 versus Treatment 1)

3.5.1. Differentially expressed genes

A total 1086 genes are differentially expressed; 507 were upregulate while 579 were downregulated in SAHA derived adipocytes. Top 20 significantly differentially expressed genes are shown in table 5. All of the differentially expressed genes between the two treatments are listed in supplementary information 2.

3.5.2. GO enrichment analysis

Non-redundant GO terms, post semantics similarity, that are significantly over represented in the list of up and down regulated genes in adipocytes derived with SAHA are shown in Fig. 7A and B respectively.

3.5.3. Pathway enrichment analysis

Pathway enrichment analysis identified 16 significantly (≤0.05 FDR) overrepresented pathways in the Reactome database for down regulated genes in adipocytes derived with SAHA (Fig. 8). However, for the upregulated genes in SAHA derived adipocytes no pathways were significantly enriched.

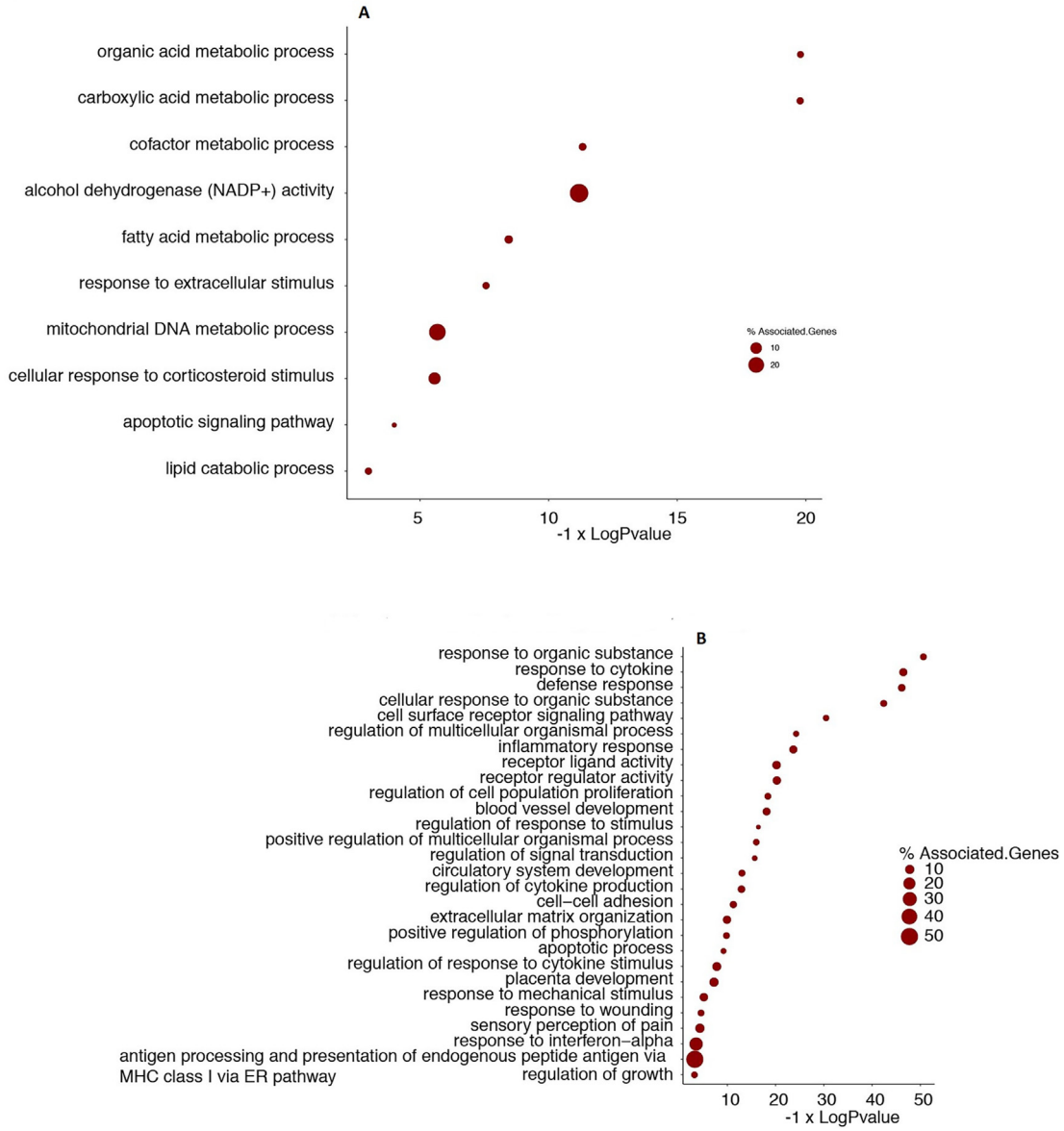

Fig. 7. (A) GO terms enriched in upregulated genes in adipocytes derived with Treatment 2 (SAHA) versus Treatment 1 (5-aza) derived adipocytes. Hypergeometric test was performed on the upregulated genes in adipocytes derived with SAHA to find GO terms that are significantly enriched. They are shown in y-axis and the associated adjusted p-value (Bonferroni step down) are reported in x-axis. Size of the dots shows the percentage of genes associated with the GO term identified in the up-regulated genes. (B) GO terms enriched in downregulated genes in adipocytes derived with Treatment 2 (SAHA) versus Treatment 1 (5-aza) derived adipocytes. Hypergeometric test was also performed on down regulated genes to find statistically significant GO terms. These GO terms are shown in y-axis and the associated adjusted p-value (Bonferroni step down) are reported in x-axis. Size of the dots represent the percentage of genes associated with the GO term identified in the down-regulated genes in SAHA derived adipocytes.

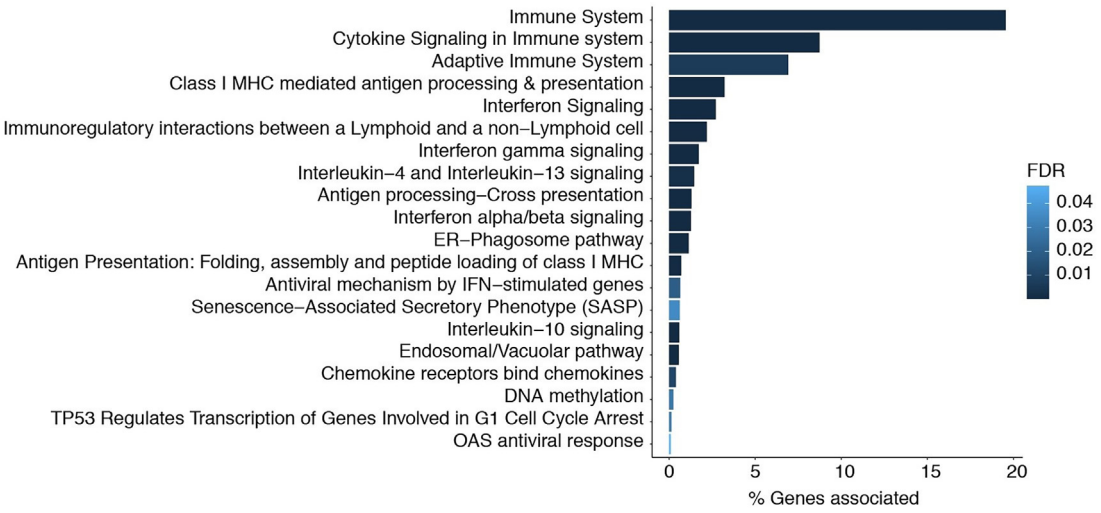

Fig. 8. Pathway enrichment in upregulated genes in adipocytes derived with Treatment 2 (SAHA) versus Treatment 1 (5-aza) derived adipocytes. Shown are the pathways in Reactome database significantly enriched for downregulated genes in Treatment 2 (SAHA). Pathway names are shown in the y-axis and the percentage of genes associated with the enriched pathway are reported in the x-axis. Colour gradient corresponds to FDR.

3.5.4. Transcription factor analysis

A total 49 of transcription factors (TFs) are differentially expressed between 5-aza derived adipocytes and SAHA derived adipocytes. Unsupervised clustering of TFs (Fig. 9) shows that the samples within the group are consistent in expression and the samples cluster in accordance with the group.

3.6. Summarizing DEs across all the sample comparison

We further assessed the common and uniquely differently expressed genes across all the comparisons.

Fig. 10 shows that there is some overlap between the up and down-regulated genes of 5-aza derived adipocytes versus control adipocytes and SAHA derived adipocytes versus control adipocytes (jaccard score 0.34) as well as between the down and up-regulated genes of 5-aza derived adipocytes versus control adipocytes and 5-aza derived adipocytes versus SAHA derived adipocytes (jaccard score 0.33).

3.7. Summarizing differentially expressed transcription factors

We assessed the common and uniquely differently expressed transcription factors (TFs) across all the comparisons (Fig. 11) and observed some overlap between the over and under-expressed TFs of 5-aza derived adipocytes versus control adipocytes and SAHA derived adipocytes versus control adipocytes (jaccard score 0.3) as well as between the under and over-expressed genes of 5-aza derived adipocytes versus control adipocytes and 5-aza derived adipocytes versus SAHA derived adipocytes (jaccard score 0.29).

4. Discussion

The transcriptomic profiles revealed that 5-aza treatment regulated vast number of genes which, in turn, inhibited the adipogenic differentiation of MG-63 cells. While SAHA treatment do not regulate many genes but it enhanced the adipogenic differentiation of MG-63 cells compared to control. It is known that 5-aza demethylate the genome and regulate genes. We have previously reported that 5-aza inhibit the adipogeneic differentiation of the MG-63 cells (El-Serafi et al., 2019). In this study, we have assessed the changes in genes expression according to our treatments, through a transcriptomic analysis approach. These epigenetic modifiers regulate the cellular differentiation. The differentiation of MSCs into osteoblasts and adipocytes are antagonizing events; a switch to either lineage will inhibit the other linage differentiation (Li et al., 2018). One study reported the inhibition of adipogenesis with the treatment of 3T3 cells with 5-aza (Chen et al., 2016). Other studies reported that DNA demethylation enhances the osteoblastic differentiation of Human Periodontal Ligament Stem Cells (Liu et al., 2016), as well as bone marrow derived stromal cells (El-Serafi et al., 2011), suggesting that DNA methylation may inhibit the adipogenic differentiation of the same cells.

Our transcriptomics study revealed that 5-aza regulates vast number of genes during the inhibition of adipogenic differentiation of MG-63 cells. Furthermore, the GO terms enriched in the upregulated genes in 5-aza derived adipocytes do not contain any adipogenesis related processes, confirming the reported adipopgenic inhibition (Fig. 3A). On contrary, the GO terms enriched in the down-regulated genes in adipocytes derived with the 5-aza contained adipogenesis related GO terms such as neutral lipid biosynthetic process, carboxylic acid metabolic processes, lipid metabolic processes, cellular amide metabolic processes and cellular carbohydrate metabolic processes (Fig. 3B). The genes enlisted in these GO terms (supporting information 2) are down regulated in 5-aza derived adipocytes compared with control adipocytes. All of these genes are involved in metabolism which is a key characteristic of adipocytes. It is not possible to describe the functions of all of these gene listed in these specific enriched GO terms. However, to illustrate the significance of these genes, we chose to elaborate more the key genes in GO term of neutral lipid biosynthetic process: ANG, DGAT2, FITM2, NR1H3, PCK1, PCK2, PLCE1 and SLC27A1 (supplementary information 2). All of these genes, downregulated in 5-aza-derived adipocytes, are involved in lipid biosynthesis. One of the main gene Diacylglycerol O-acyltransferases (DGAT2) is involved in triacylglycerol metabolism (Bhatt-Wessel et al., 2018). While FITM2 (Fat Storage Inducing Transmembrane Protein 2) is a storage protein and its abundance is affected in type 2 diabetes (Agrawal et al., 2019). The two isoforms PCK1 and 2 of phosphoenolpyruvate carboxy kinase are involved in the gluconeogenesis; these enzymes are dysregulated in the obesity and diabetes (Beale et al., 2007). Literature review of other genes listed in the GO terms of carboxylic acid metabolic processes, lipid

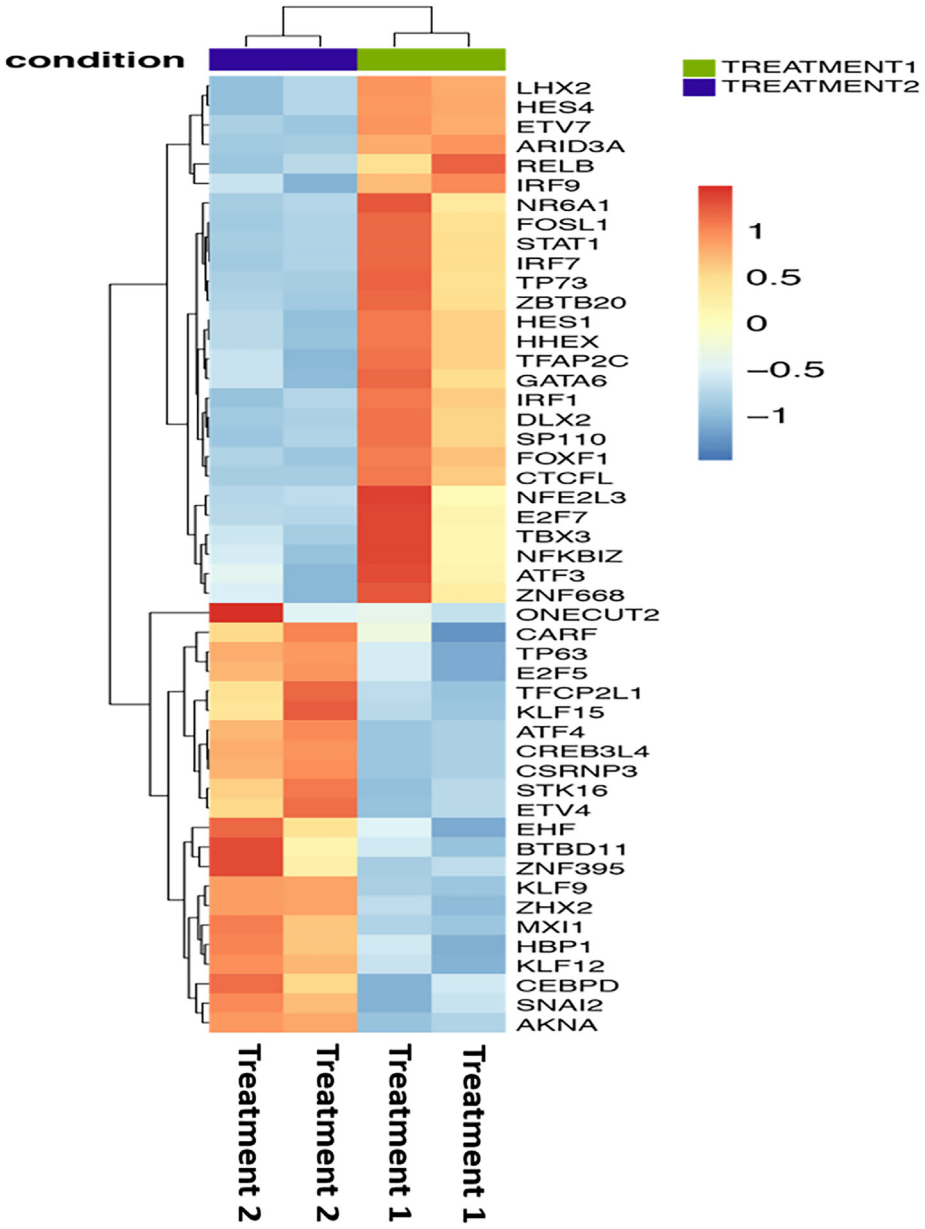

Fig. 9. Hierarchical clustering of differentially expressed transcription factors between Treatment 1 (5-aza) and Treatment 2 (SAHA) derived adipocytes. Statistically significant transcription factors are shown between SAHA and 5-aza derived adipocytes. The color scale bar indicates z-score values after normalization. Heatmap was generated using heatmap package from R.

metabolic processes, cellular amide metabolic processes and cellular carbohydrate metabolic processes reveal more adipogenic related information. In the subset of these differentially expressed genes there are specific transcription factors which should be studied further to completely understand the adipogenic differentiation (Figs. 6 and 9). Although there are some overlaps among the differentially expressed genes in these sets (Figs. 10 and 11), the vast majorities of the differentially expressed genes are unique to the specific sets.

GSEA was also performed on MAP kinase and PI3-akt pathways, as these pathways were involved in enhanced adipogenesis, as shown in our early study (Fayyad et al., 2019). The GSEA showed that both pathways were upregulated in adipocytes derived with 5-aza treatment (Fig. 4), contrary to our finding in a previous study. However, in the previous study, adipogenic differentiation of immortalized human mesenchymal stromal cells (iMSC3) was studied. Hence, it can be concluded that the antagonizing roles of the two pathways during the adipogenesis is due to the different nature of the two cell types. Same signaling pathways may have different even antagonizing effects in different cells. A study on pancreatic cancer has also showed a role for DNA methylation in the regulation of MAP-kinase pathway (Wang et al., 2013). Another study has also revealed that DNA methylation upregulate the PI-3 kinase and ERK1 pathways in human fibrosarcoma (Yu and Kim, 2016). In our study the DNA demethylation of MG-63, using our application protocol, would have affected these pathways as these pathways were upregulated in the adipocytes derived with the 5-aza treatment. These pathways, in this context, would have inhibited the adipogenic differentiation of MG-63 cells. The KEGG pathways enriched in the upregulated genes in 5-aza derived adipocytes do not have any pathway that is involved in lipogenesis (Fig. 5). The transcription factors that are differentially regulated between control adipocytes and 5-aza derived adipocytes would regulate the adipogenic differentiation (Fig. 6). These differentially

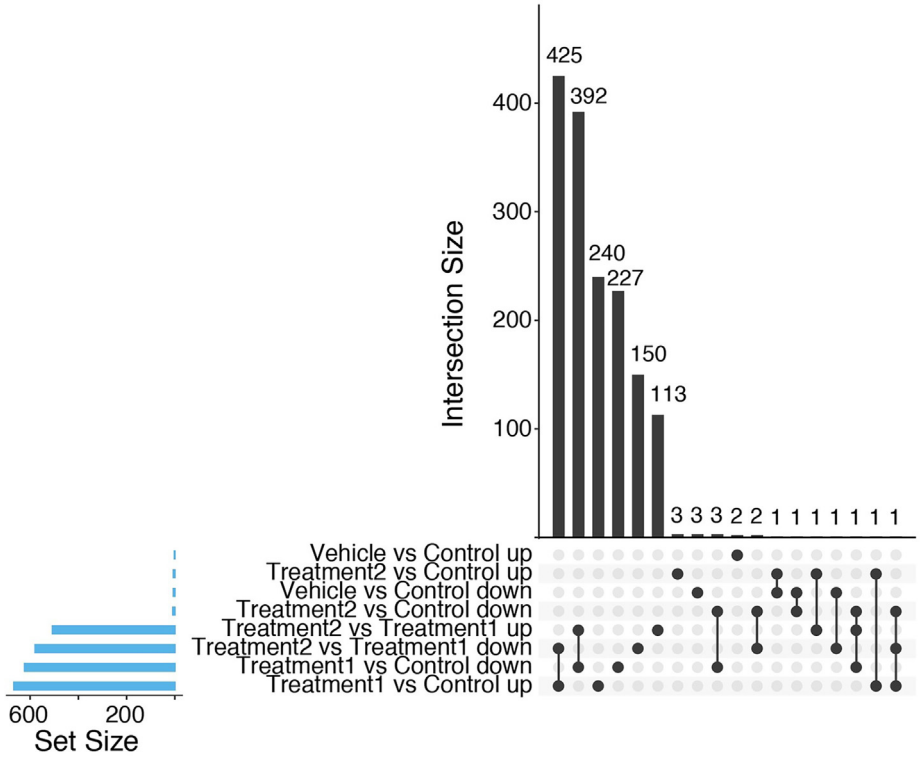

Fig. 10. UpSet plot of intersection across the comparisons. On the left, for each comparison the total number of up and down regulated genes are shown. The bar chart above shows the size of interaction between sets of genes in each comparison. The connected dots on the bottom panel show the comparisons considered for each intersection.

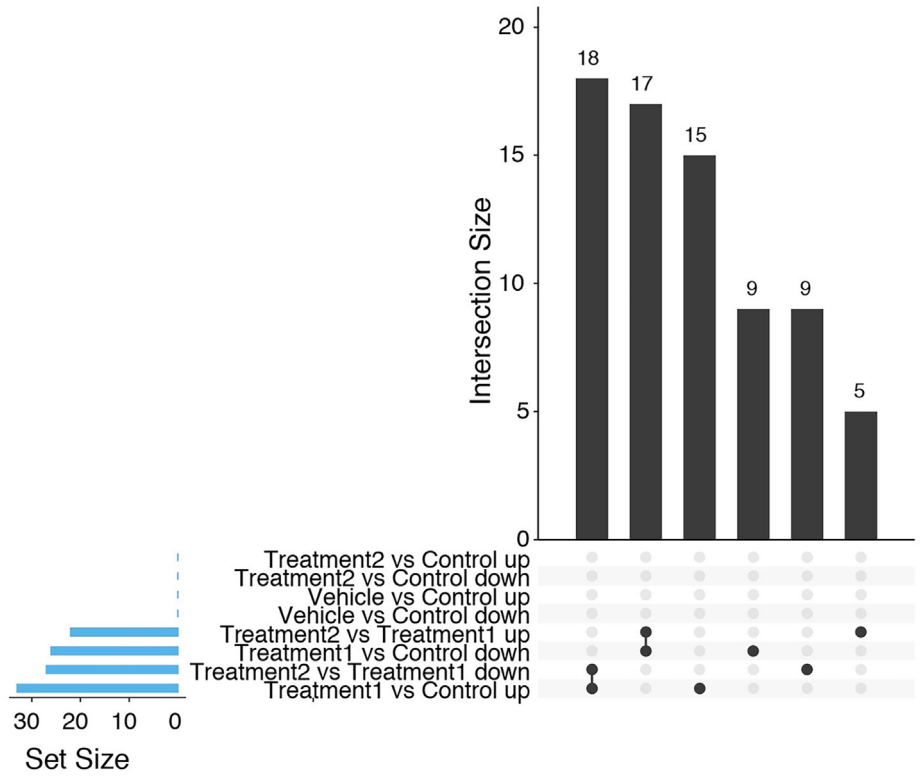

Fig. 11. UpSet plot of intersection across the comparisons. The bar chart on the left shows the total number of genes for each comparison separately for over and under expressed transcription factors (TFs). The upper bar chart shows the size of intersection between sets of TFs up / down-expressed with one or more comparisons. The connected dots on the bottom panel show the comparisons considered for each intersection.

expressed transcription factors should be further investigated for their roles in adipogenesis as most of these differentially regulated transcription factors will likely have roles in adipogenesis.

SAHA treatment enhanced the adipogenic differentiation of MG-63 cells. SAHA inhibits histone deacetylation and consequently enhances the adipogenic differentiation of MG-63 cells. The enhanced adipocytes derived with SAHA do not have that many differentially expressed genes compared with control adipocytes. However, it is known that HDAC inhibitors regulate cellular processes such as cell cycle, apoptosis, cell signaling pathways, etc. (Eckschlager et al., 2017). These pathways affect the cellular differentiation. Surprisingly, only 14 genes were differentially regulated in SAHA derived adipocytes, according to our treatment protocol, and neither any GO term nor any KEGG pathway was significantly enriched. However, these 14 differentially expressed genes between SAHA derived adipocytes and control might have enhanced the adipogenic differentiation of MG-63 cells. Furthermore, this study was focused on differential regulation of genes due to 5-aza and SAHA treatments; the sequencing was performed to sequence the genes not microRNAs. Further study on differential regulation of micoRNAs and proteins will likely reveal key regulators (proteins and microRNAs) that may be involved in the enhanced adipogenic differentiation of MG-63. Hence, proteins and miroRNAs expression profiles of the control adipocytes and SAHA derived adipocytes should be compared in a future study to find key regulators other than genes that enhances the differentiation. We hypothesize that SAHA might have more potent effects on the regulations of proteins and microRNAs.

DMSO was used as a vehicle to dissolve 5-aza and SAHA. To analyze the effects of DMSO on the gene regulation, the transcriptomes of the vehicle derived adipocytes and the control adipocytes were compared. Although the vehicle did not regulate the adipogenesis, but it affected the transcription of 8 genes during differentiation. It indicates the DMSO has non-specific effects on gene activity, which has been previously reported in several studies (Thaler et al., 2012; Sumida et al., 2011).

To confirm the vast changes of the transcriptome due to 5-aza treatment, we also compared the transcriptomics profiles of 5-aza derived and SAHA derived adipocytes. As the SAHA treatment did not regulate many genes, the comparison revealed similar vast changes in the transcriptome as that of vast changes in the transcriptome of control and 5-aza. Additional information 2 contains all of the differentially regulated genes and GO terms are listed for all comparisons.

The vast number of these genes including transcription factors that are differentially regulated due to the 5-aza can be used as potential markers for inhibition of adipogenesis, particularity obesity treatment. However, further research is needed to ascertain their roles as inhibitory agents.

5. Conclusion

The DNA methylation inhibitor 5-aza inhibits the adipogenic differentiation of MG-63 cells by regulation vast number of genes including several transcription factors. This differential expression of genes should be further assessed for their roles in adipogenesis which may lead to their use as obesity markers. SAHA, on the other hand, affects a small group of genes and enhances the adipogenic differentiation. This limited, but effective, action would have another advantage of safety which increases the chance of SAHA based protocol for enhancing the adipogenic differentiation to be applied clinically. However, further microRNAs sequencing and proteomic studies of the control and SAHA derived adipocytes will lead to identification of more key regulators (proteins and microRNAs) that enhance the adipogenesis.

Funding

The authors would like to thank Al Jalila Foundation (grant no. AJF201533) and Sheikh Hamdan Bin Rashid Al Maktoum Award for Medical Sciences (Grant no.: MRG-6112013-2014) for funding this project.

Declaration of Competing Interest

The authors declare that they have no known competing financial interests or personal relationships that could have appeared to influence the work reported in this paper.

Appendix A. Supplementary material

Supplementary data to this article can be found online at https://doi.org/10.1016/j.sjbs.2021.08.033.

References

Agrawal, M., Yeo, C.R., Shabbir, A., Chhay, V., Silver, D.L., Magkos, F., Vidal-Puig, A., Toh, S.-A., 2019. Fat storage-inducing transmembrane protein 2 (FIT2) is less abundant in type 2 diabetes, and regulates triglyceride accumulation and insulin sensitivity in adipocytes. FASEB J. 33 (1), 430–440. https://doi.org/10.1096/fsb2.v33.110.1096/fj.201701321RR.

Beale, E.G., Harvey, B.J., Forest, C., 2007. PCK1 and PCK2 as candidate diabetes and obesity genes. Cell Biochem. Biophys. 48 (2-3), 89–95. https://doi.org/10.1007/s12013-007-0025-6.

Bhatt-Wessel, B., Jordan, T.W., Miller, J.H., Peng, L., 2018. Role of DGAT enzymes in triacylglycerol metabolism. Arch. Biochem. Biophys. 655, 1–11. https://doi.org/10.1016/j.abb.2018.08.001.

Bindea, G., Mlecnik, B., Hackl, H., Charoentong, P., Tosolini, M., Kirilovsky, A., et al., 2009. ClueGO: a Cytoscape plug-in to decipher functionally grouped gene ontology and pathway annotation networks. Bioinformatics. 25, 1091-1093. doi: 10.1093/bioinformatics/btp101

Blaheta, R.A., Cinatl, J., 2002. Anti-tumor mechanisms of valproate: a novel role for an old drug. Med. Res. Rev. 22 (5), 492–511. https://doi.org/10.1002/med.10017.

Chawla, K., Tripathi, S., Thommesen, L., Lægreid, A., Kuiper, M., 2013. TFcheckpoint: a curated compendium of specific DNA-binding RNA polymerase II transcription factors. Bioinformatics 29, 2519–2520. https://doi.org/10.1093/bioinformatics/btt432.

Chen, J., Gao, Y., Huang, H., Xu, K., Chen, X., Jiang, Y., Li, H., Gao, S., Tao, Y.u., Wang, H., Zhang, Y., Wang, H., Cai, T., Gao, S., 2015. The combination of Tet1 with Oct4 generates high-quality mouse-induced pluripotent stem cells. Stem Cells. 33 (3), 686–698. https://doi.org/10.1002/stem.1879.

Chen, Y.-S., Wu, R., Yang, X., Kou, S., MacDougald, O.A., Yu, L., Shi, H., Xue, B., 2016. Inhibiting DNA methylation switches adipogenesis to osteoblastogenesis by activating Wnt10a. Sci. Rep. 6 (1). https://doi.org/10.1038/srep25283.

Dobin, A., Davis, C. A., Schlesinger, F., Drenkow, J., Zaleski, C., Jha, S., et al., 2013. STAR: ultrafast universal RNA-seq aligner. Bioinformatics. 29, 15-21. doi: 10.1093/bioinformatics/bts635

Eckschlager, T., Plch, J., Stiborova, M., Hrabeta, J., 2017. Histone Deacetylase Inhibitors as Anticancer Drugs. Int. J. Mol. Sci. 18 (7), 1414. https://doi.org/10.3390/ijms18071414.

El-Serafi, A.T., Oreffo, R.O.C., Roach, H.I., 2011. Epigenetic modifiers influence lineage commitment of human bone marrow stromal cells: Differential effects of 5-aza-deoxycytidine and trichostatin A. Differentiation. 81 (1), 35–41. https://doi.org/10.1016/j.diff.2010.09.183.

El-Serafi, A.T., Sandeep, D., Abdallah, S., Lozansson, Y., Hamad, M., Khan, A.A., 2019. Paradoxical effects of the epigenetic modifiers 5-aza-deoxycytidine and suberoylanilide hydroxamic acid on adipogenesis. Differentiation. 106, 1–8. https://doi.org/10.1016/j.diff.2019.02.003.

Elsharkawi, I., Parambath, D., Saber-Ayad, M., Khan, A.A., El-Serafi, A.T., 2020. Exploring the effect of epigenetic modifiers on developing insulin-secreting cells. Hum. Cell 33 (1), 1–9. https://doi.org/10.1007/s13577-019-00292-y.

Fabregat, A., Sidiropoulos, K., Viteri, G., Forner, O., Marin-Garcia, P., Arnau, V., D'Eustachio, P., Stein, L., Hermjakob, H., 2017. Reactome pathway analysis: a high-performance in-memory approach. BMC Bioinf. 18 (1). https://doi.org/10.1186/s12859-017-1559-2.

Fayyad, A., Khan, A., Abdallah, S., Alomran, S., Bajou, K., Khattak, M., 2019. Rosiglitazone Enhances Browning Adipocytes in Association with MAPK and PI3-K Pathways During the Differentiation of Telomerase-Transformed Mesenchymal Stromal Cells into Adipocytes. Int. J. Mol. Sci. 20 (7), 1618. https://doi.org/10.3390/ijms20071618.

Higuchi, A., Ling, Q.-D., Kumar, S.S., Munusamy, M.A., Alarfaj, A.A., Chang, Y., Kao, S.-H., Lin, K.-C., Wang, H.-C., Umezawa, A., 2015. Generation of pluripotent stem

cells without the use of genetic material. Lab Invest. 95 (1), 26–42. https://doi.org/10.1038/labinvest.2014.132.
Jones, P.A., Takai, D., 2001. The role of DNA methylation in mammalian epigenetics. Science 293, 1068–1070. https://doi.org/10.1126/science.1063852.
Khan, A.A., Huat, T.J., Al Mutery, A., El-Serafi, A.T., Kacem, H.H., Abdallah, S.H., Reza, M.F., Abdullah, J.M., Jaafar, H., 2020. Significant transcriptomic changes are associated with differentiation of bone marrow-derived mesenchymal stem cells into neural progenitor-like cells in the presence of bFGF and EGF. Cell Biosci. 10 (1). https://doi.org/10.1186/s13578-020-00487-z.
Kim, H., Bae, S., 2011. Histone deacetylase inhibitors: molecular mechanisms of action and clinical trials as anti-cancer drugs. Am. J. Transl. Res. 3, 166–179.
Li, B., Dewey, C.N., 2011. RSEM: accurate transcript quantification from RNA-Seq data with or without a reference genome. BMC Bioinf. 12, 323. https://doi.org/10.1186/1471-2105-12-323.
Li, Y., Jin, D., Xie, W., Wen, L., Chen, W., Xu, J., Ding, J., Ren, D., 2018. PPAR-γ and Wnt Regulate the Differentiation of MSCs into Adipocytes and Osteoblasts Respectively. Curr. Stem. Cell Res. Ther. 13 (3), 185–192. https://doi.org/10.2174/1574888X12666171012141908.
Liu, Z., Chen, T., Sun, W., Yuan, Z., Yu, M., Chen, G., Guo, W., Xiao, J., Tian, W., 2016. DNA Demethylation Rescues the Impaired Osteogenic Differentiation Ability of Human Periodontal Ligament Stem Cells in High Glucose. Sci. Rep. 6 (1). https://doi.org/10.1038/srep27447.
Love, M.I., Huber, W., Anders, S., 2014. Moderated estimation of fold change and dispersion for RNA-seq data with DESeq2. Genome Biol. 15, 550. https://doi.org/10.1186/s13059-014-0550-8.
Mariadason, J.M., Corner, G.A., Augenlicht, L.H., 2000. Genetic reprogramming in pathways of colonic cell maturation induced by short chain fatty acids: comparison with trichostatin A, sulindac, and curcumin and implications for chemoprevention of colon cancer. Cancer Res. 60, 4561–4572.
Roth, S.Y., Allis, C.D., 1996. Histone acetylation and chromatin assembly: a single escort, multiple dances? Cell 87 (1), 5–8. https://doi.org/10.1016/S0092-8674(00)81316-1.
Sandor, V., Senderowicz, A., Mertins, S., Sackett, D., Sausville, E., Blagosklonny, M.V., Bates, S.E., 2000. P21-dependent G 1 arrest with downregulation of cyclin D1 and upregulation of cyclin E by the histone deacetylase inhibitor FR901228. Br. J. Cancer 83 (6), 817–825. https://doi.org/10.1054/bjoc.2000.1327.
Shannon, P., Markiel, A., Ozier, O., Baliga, N.S., Wang, J.T., Ramage, D., et al., 2003. Cytoscape: a software environment for integrated models of biomolecular interaction networks. Genome Res. 13, 2498–2504. https://doi.org/10.1101/gr.1239303.
Subramanian, A., Tamayo, P., Mootha, V.K., Mukherjee, S., Ebert, B.L., Gillette, M.A., Paulovich, A., Pomeroy, S.L., Golub, T.R., Lander, E.S., Mesirov, J.P., 2005. Gene set enrichment analysis: a knowledge-based approach for interpreting genome-wide expression profiles. Proc. Natl. Acad. Sci. USA 102 (43), 15545–15550. https://doi.org/10.1073/pnas.0506580102.
Sumida, K., Igarashi, Y., Toritsuka, N., Matsushita, T., Abe-Tomizawa, K., Aoki, M., Urushidani, T., Yamada, H., Ohno, Y., 2011. Effects of DMSO on gene expression in human and rat hepatocytes. Hum. Exp. Toxicol. 30 (10), 1701–1709. https://doi.org/10.1177/0960327111399325.
Thaler, R., Spitzer, S., Karlic, H., Klaushofer, K., Varga, F., 2012. DMSO is a strong inducer of DNA hydroxymethylation in pre-osteoblastic MC3T3-E1 cells. Epigenetics. 7 (6), 635–651. https://doi.org/10.4161/epi.20163.
Wang, X., Wang, H., Jiang, N., Lu, W., Zhang, X.F., Fang, J.Y., 2013. Effect of inhibition of MEK pathway on 5-aza-deoxycytidine-suppressed pancreatic cancer cell proliferation. Genet. Mol. Res. 12, 5560–5573. https://doi.org/10.4238/2013.November.18.6.
Yu, S., Kim, S.J., 2016. 5-Azacytidine regulates matrix metalloproteinase-9 expression, and the migration and invasion of human fibrosarcoma HT1080 cells via PI3-kinase and ERK1/2 pathways. Int. J. Oncol. 49, 1241–1247. https://doi.org/10.3892/ijo.2016.3612.
Yuan, P., Huang, L., Jiang, Y., Gutkind, J. S., Manji, H. K., and Chen, G., 2001. The Mood Stabilizer Valproic Acid Activates Mitogen-activated Protein Kinases and Promotes Neurite Growth*. J. Biol. Chem. 276, 31674-31683. doi: 10.1074/jbc.M104309200